

Earth and Space Science



RESEARCH ARTICLE

10.1029/2019EA000898

Performance of GNSS Global Ionospheric Modeling Augmented by LEO Constellation

Xiaodong Ren^{1,2,3}, Xiaohong Zhang^{1,4,5}, Michael Schmidt², Zhibo Zhao¹, Jun Chen^{1,4}, Jincheng Zhang¹, and Xingxing Li¹

Key Points:

- LEO satellite was utilized for global ionosphere modeling
- LEO satellite observations can fill the gap of missing spatial and temporal values in existing GNSS-based ionospheric modeling
- By combining LEO constellation and Multi-GNSS simulated datasets, higher accuracy and higher spatial model can be achieved

¹School of Geodesy and Geomatics, Wuhan University, Wuhan, China, ²Deutsches Geodätisches Forschungsinstitut der Technischen Universität München (DGFI-TUM), Munich, Germany, ³Key Laboratory of Geospace Environment, University of Science & Technology of China, Chinese Academy of Sciences, Hefei, China, ⁴Key Laboratory of Geospace Environment and Geodesy, Ministry of Education, Wuhan, China, ⁵Collaborative Innovation Center for Geospatial Technology, Wuhan, China

Correspondence to:

X. Ren,
renxiaodongfly@gmail.com

Citation:

Ren, X., Zhang, X., Schmidt, M., Zhao, Z., Chen, J., Zhang, J., & Li, X. (2020). Performance of GNSS global ionospheric modeling augmented by LEO constellation. *Earth and Space Science*, 7, e2019EA000898. <https://doi.org/10.1029/2019EA000898>

Received 17 SEP 2019

Accepted 20 NOV 2019

Accepted article online 13 DEC 2019

Abstract The Low-Earth-Orbiting (LEO) satellite has a fast motion and thus contributes to rapid changes in satellite geometric distribution, which can effectively mitigate multipath effects and offer more available observations. Recently, some studies have investigated LEO-augmented Global Navigation Satellite System (GNSS) positioning and navigation. However, the study of LEO-augmented global ionospheric modeling was not yet available. In this paper, we present the performance and accuracy of global ionospheric model augmented by LEO constellation for the first time. Based on the three kinds of designed LEO constellations with 60, 96, and 192 satellite simulation data, the results show that LEO observations can expand the coverage and increase the density of ionospheric pierce points (IPPs). Meanwhile, the density of IPPs becomes higher with an increasing number of LEO satellites. When the cutoff elevation is set to 40°, the IPP distribution of GNSS+LEO is still better than that of GNSS-only at 10°. This way the cutoff elevation angle of the GNSS measurements can be increased, since the mapping function error and the multipath effects are reduced. Furthermore, the performances of global ionosphere maps based on the observations of GNSS-only and GNSS+LEO scenarios are evaluated. Compared with GNSS-only, the minimum and maximum bias can be reduced from -18.1 to -7.0 total electron content unit and from 12.6 to 6.4 total electron content unit, respectively, and the root-mean-square values with LEO constellations of 60, 96, and 192 satellites improve by 35.9%, 46.5%, and 50%, respectively.

1. Introduction

The Global Navigation Satellite System (GNSS) has been widely used to monitor the ionosphere due to its high accuracy, temporal and spatial resolution, and continuous monitoring either on a regional scale or on a global scale (Feltens & Schaer, 1998; Hernández-Pajares et al., 2011; Lanyi & Roth, 1988; Mannucci et al., 1993; Ren et al., 2019; Schaer, 1999; Wang et al., 2018; Yuan & Ou, 2002). With the completion of Beidou, Galileo, and the establishment of many other regional navigation systems, the number of available navigation satellites will be larger than 120 in combination with Global Positioning System (GPS) and Global Navigation Satellite System (GLONASS). This can provide more observations for ionospheric modeling than ever (Ren et al., 2016; Yao et al., 2018; Abdelazeem et al., 2017; Zhang et al., 2015). However, the performance of GNSS-based ionospheric model still highly depends on the number of ground-based stations and their distribution. Note that there are only a few monitoring stations over areas with harsh natural conditions, for example, Northern Africa, the polar regions as well as the oceans, leading to the low accuracy and unreliability of ionospheric models over these regions. To improve the accuracy and reliability of the ionospheric model on a global scale, some research groups start to model the ionosphere combined with the observations of altimetry satellites such as the Jason missions, radio occultation from the Constellation Observing System for Meteorology, Ionosphere, and Climate (COSMIC) mission and tracking data from the Doppler Orbitography and Radiopositioning Integrated by Satellite (DORIS) system (Alizadeh et al., 2011; Chen et al., 2017; Dettmering et al., 2014; Hu et al., 2019; Li et al., 2012; Todorova et al., 2008). However, the improvement is not very obvious due to the limited number of satellites.

The rapid development of LEO satellite constellations provides a potential opportunity to solve the above-mentioned problem. The earliest LEO satellite constellation was launched by the United States in the late

© 2019 The Authors.

This is an open access article under the terms of the Creative Commons Attribution License, which permits use, distribution and reproduction in any medium, provided the original work is properly cited.

1990s consisting of 66 polar-orbiting satellites, which is of about 2 times larger than that of GPS. Nevertheless, users could only observe one LEO satellite at the same time not leading to a performance enhancement of GNSS PNT (position, navigation and timing). As a result, some of the world's leading scientific and commercial institutions are preparing for the next generation of LEO satellite constellation. In January 2015, Onweb announced a partnership with Virgin and Qualcomm to launch a constellation of 648 LEO satellites in 2020 for broadband Internet transmission worldwide (Hanson, 2016). Boeing, SpaceX, Samsung, and other companies have also proposed their own LEO satellite constellation plans, and the number of satellites designed has reached more than 3,000–4,000 (Selding, 2015a, 2015b, 2016; Reid et al., 2016). Up to now, nearly 20 famous institutions and enterprises have announced their LEO satellite launch plans. It is expected that the number of available LEO satellites in the air will reach hundreds or even thousands after the completion of the plans. Among them, some LEO satellite constellations will also provide navigation enhancement service. Taking the “Hongyun” and “Hongyan” systems as an example, they are developed by China Aerospace Science and Technology Corporation and Aerospace Science and Technology Industry Group, respectively (Li et al., 2019). The first experimental satellite has been launched by the end of 2018, and constellations composed of more than 150 and 300 LEO satellites are planned to be launched in 2022 and 2024, respectively. When these projects are completed, the constellations can be used to provide access to internet transmission worldwide as well as enhance the global PNT service.

In recent years, some scholars have begun to carry out relevant research studies on LEO-augmented GNSS precise orbit determination and positioning. Reid et al. (2016) proposed to extend the application of commercial LEO constellation to GPS navigation enhancement and demonstrated its feasibility. The results show that LEO constellation can effectively enhance PNT services. Lawrence et al. (2016) tested the effect of Iridium system on timing and location services, indicating that Iridium's LEO-based service can significantly enhance the capability of GNSS, especially in areas where GNSS signals are uncovered. Li et al. (2019) investigated the precise point positioning (PPP) performance of the LEO-augmented full operational capability multi-GNSS based on simulated data. The results show that LEO-augmented GNSS can significantly improve the accuracy of orbit and PPP. Using the simulated onboard LEO data, the orbit accuracy of multi-GNSS can reach 3.3, 2.7, and 2.6 cm in radial, along-track, and cross-track components, respectively. For LEO-augmented GPS- and BDS-only PPP solutions, the convergence time can be significantly shortened by 90% from about 25 to within 3 min with a 192- or 288-satellite LEO satellite constellation.

Above all, LEO satellite constellation shows great significance in improving the accuracy of GNSS orbit determination and positioning as well as accelerating PPP convergence. Meanwhile, LEO satellite constellation with hundreds of satellites provides a large number of observations to establish ionosphere model with a high accuracy. However, the study of LEO-augmented global ionosphere mapping was not yet available. In this contribution, we will present the performance of GNSS-based global ionospheric modeling augmented by LEO constellation for the first time. Detailed studies on LEO satellite orbit simulation, LEO-based ionospheric observation simulation, and global ionospheric modeling method and strategy are shown in section 2. Afterward, we carefully analyze the distribution characteristics of ionospheric pierce point (IPP) and evaluate the accuracy of global ionospheric model with different solutions based on simulated observations in section 3. Finally, conclusions and the outlook are summarized in section 4.

2. Materials and Methods

Since many LEO constellations are still under development, there are no available observations from LEO constellations at present. In order to evaluate the contributions and advantages of LEO constellation to global ionospheric modeling, first, we need to obtain LEO-based ionospheric observations through simulation, and then conduct global ionospheric modeling by combining GNSS-based ionospheric observations, and evaluate its accuracy. The detailed processing strategies of the constellation simulation and the ionospheric observation simulation will be introduced in the following.

2.1. Data Simulation

To evaluate the impact of the satellite number of LEO constellation on global ionospheric modeling, three types of LEO constellations of 60, 96, and 192 satellites are designed in this paper. Detailed orbital configurations of the three LEO constellations are listed in Table 1. The orbital inclination is designed as 90°. The number of orbital planes is 6, 12, and 12, respectively. It is worth noting that the 60-satellite constellation

Table 1
Detailed Information of the Three Designed LEO Constellations

Sat. Num.	Plane Num.	Orbit Type	Inclination (°)
60	6	Polar satellite	90
96	12	Polar satellite	90
192	12	Polar satellite	90

has been adopted by HongYan system. Additionally, we can get a general view of the designed LEO constellations from Figure 1.

On the other hand, in order to investigate the performance of LEO-augmented GNSS ionosphere modeling with the complement of multi-GNSS in the future, this study also simulates the GNSS observations based on the full constellation of the GNSS, including GPS, GLONASS, Galileo, and BDS, as shown in Table 2. In this way, the assessment results will be

more consistent with the real situation of multi-GNSS in the future. As we can see, the total number of satellites for GPS, GLONASS, Galileo, and BDS are 24, 24, 30, and 30, respectively. Among them, the BDS constellation contains three geostationary satellites and three inclined geosynchronous orbit satellites, and the rest are 24 medium earth orbit satellites. The other three satellite systems only contain medium earth orbit satellites with an orbital altitude of about 20,000 km.

The process of ionospheric observation simulation is shown in Figure 2. The Satellite Tool Kit (STK) software (a sophisticated space-analysis platform, <http://www.agi.com/products>) is employed to simulate the orbit of both LEO satellite constellations and GNSS constellations in this study. Then we can obtain the IPPs according to the coordinates of the stations and satellites. Afterward, the ground-based GNSS slant total electron content (STEC) measurements, ground-based LEO STEC measurements, and LEO-based GNSS STEC measurements are simulated using a ionospheric electron density model (Bilitza et al., 2017; Kumar, 2016; Nava et al., 2008), for example, International Reference Ionosphere (IRI; <http://www.irimodel.org/>). In this paper, we use the latest version of IRI model, which is IRI2016 version (the download address of Fortran source code: <http://www.irimodel.org/IRI-2016/>). Finally, model the ionosphere by spherical harmonics (SH) function. Note that these simulated observations do not consider other kinds of errors, for example, the tropospheric delay, observational noise, multipath effects, clock offsets, and differential code/phrase biases. In the following, the performance of the LEO-augmented ionosphere model is evaluated in different aspects, for example, the distribution of IPPs and the modeling accuracy.

Based on LEO satellites, we can not only acquire observations from GNSS satellites through LEO-based GNSS receiver but also receive navigation-enhanced signals from LEO satellites through GNSS ground stations. Figure 3 is the schematic diagram of the mechanism of LEO-augmented GNSS observation. It indicates that LEO satellite can not only perform as a GNSS receiver to receive GNSS signals, monitoring ionosphere upside, but also can observe the bottomside of the ionosphere between ground stations and LEO satellites. Here the Figure 4a shows the global distribution of GNSS ground-based stations and Figures 4b–4d are the global distribution of LEO satellite-based stations with 60, 92, and 192 LEO satellites, respectively. As is shown in the figure, GNSS ground-based stations are mostly located in continents, especially in Europe, while there are few in the oceans. On the contrary, LEO satellite-based stations have a better distribution, evenly distributed on the Earth's surface. And with the increasing number of LEO satellite, which is 60, 96, and 192, respectively, the density of LEO satellite-based stations is getting higher.

2.2. Ionosphere Modeling

As is shown in Figure 3 that there are three types of observables according to the relationship between GNSS ground-based monitoring stations, LEO satellites, and GNSS satellites. In this study, we can simulate these

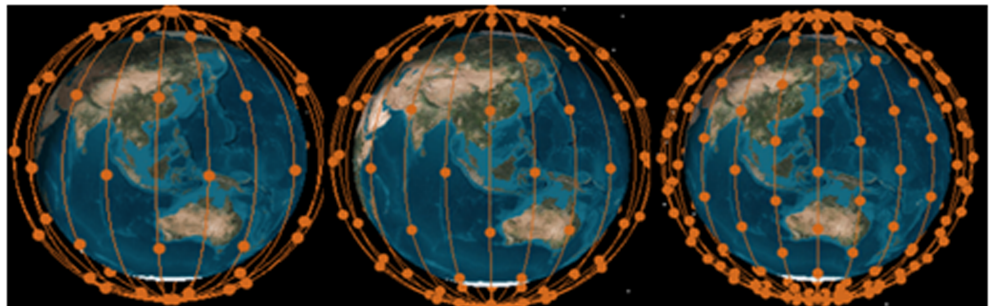


Figure 1. Designed Low-Earth-Orbiting (LEO) constellations: (left) 60 LEO satellites, (middle) 96 LEO satellites, and (right) 192 LEO satellites.

Table 2
Detailed Information of Simulated GNSS Constellations

Satellite System	GPS	GLONASS	Galileo	BDS MEO	BDS GEO	BDS IGSO
Sat. num.	24	24	30	24	3	3
Inclination (°)	56	64.8	56	55	0	55
Altitude (km)	20,180	19,100	23,220	21,528	35,786	35,786

Abbreviations: GEO: geostationary satellites; GLONASS: Global Navigation Satellite System; GNSS: Global Navigation Satellite System; GPS: Global Positioning System; IGSO: inclined geosynchronous orbit satellites; MEO: medium earth orbit.

three types of observations with IRI model. Once the simulated ionospheric observations from IRI are obtained, we can estimate the ionosphere model from the ionospheric observations converted by a specific ionospheric mapping function at each IPP using a specific fitting model. In this study, the ionospheric single-layer mapping function is used to convert STEC to vertical total electron content (TEC). Besides, we apply a series expansion in SH to fit the ionospheric observations on the global scale, which can be expressed as follows (Schaer, 1999):

$$MF \cdot STEC(\varphi, \lambda) = \sum_{n=0}^{n_{\max}} \sum_{m=0}^n \tilde{P}_{mn}(\sin\varphi) \left(\tilde{C}_{mn} \cos(m\lambda) + \tilde{S}_{mn} \sin(m\lambda) \right) \quad (1)$$

where MF is the ionospheric mapping function; n and m represent the degree and order of the SH expansion, respectively; n_{\max} is the largest order of the expansion of SH expansion; \tilde{P}_{mn} is the normalized associated Legendre function of degree n and order m ; φ denotes the geomagnetic or geographic latitude of the IPP; λ and λ_0 are the longitude of the IPP and the Sun, respectively; STEC (φ, λ) is the STEC value at corresponding IPP; and \tilde{C}_{mn} and \tilde{S}_{mn} are the SH coefficients have to be estimated. The detailed strategy to estimate the ionospheric key parameters in this paper is shown in Table 3.

3. Results and Discussion

Generally, the number of IPPs and their spatial distribution will affect the accuracy of the modeling significantly. In this sense, the distribution and characteristic of LEO-based IPPs compared with that of GNSS will be analyzed in this section. The performance of the estimated global ionosphere model obtained from GNSS/LEO observations will be presented as well.

3.1. Accuracy Index

For the evaluation of the accuracy of the ionosphere models estimated from GNSS-only, GNSS+LEO-BTM, and GNSS+LEO-BTM+LEO-UP, four statistical indices are used to quantify their performance, that is, the bias, the standard deviation (STD), the root-mean-square (RMS) value and the improvement (Imp). The equations are given as follows:

$$\begin{cases} \text{bias} = \langle TEC_0 - TEC_{\text{ref}} \rangle \\ STD = \sqrt{\langle TEC_0 - TEC_{\text{ref}} - \text{bias} \rangle^2} \\ RMS = \sqrt{\langle TEC_0 - TEC_{\text{ref}} \rangle^2} \\ \text{Imp} = \frac{\langle TEC_0 - TEC_{\text{ref}} \rangle}{TEC_{\text{ref}}} \end{cases} \quad (2)$$

where TEC_0 is the TEC value obtained from the estimated ionosphere model, TEC_{ref} is the reference TEC value derived from IRI GIM, and the symbol $\langle \rangle$ denotes the mean value during the chosen time period.

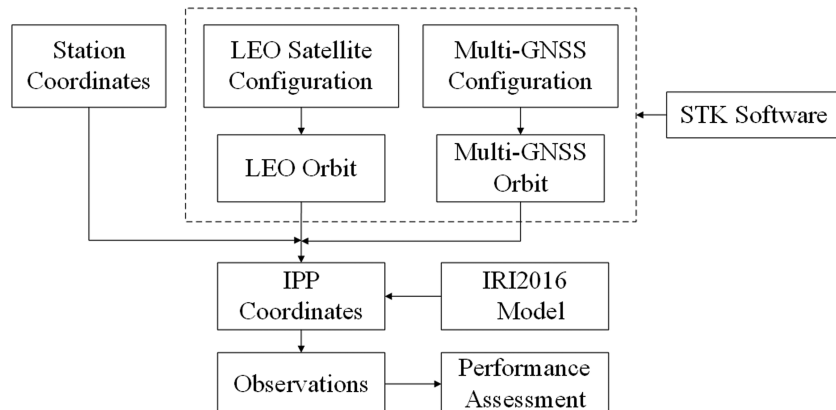


Figure 2. Flowchart of the data simulation process.

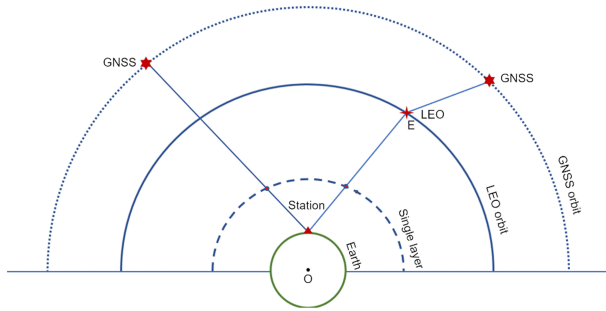


Figure 3. Schematic diagram of ionospheric top-side and bottom-side observation from Low-Earth-Orbiting (LEO) and Global Navigation Satellite System (GNSS) satellites.

3.2. Performance of the IPP Distribution

To analyze the distribution of the IPPs from the combination of LEO satellite constellations, we present the global coverage of IPPs derived from 192 LEO satellites in different length of time in Figure 5. Here the green, the red, and the blue dots represent the distribution of IPPs derived from GNSS-only, LEO-BTM, and LEO-UP, respectively. It can be seen that with the increase of observation time, the coverage and density of IPPs based on all the three solutions are becoming wider and higher. For GNSS-only, the improvement is mainly embodied in density while IPPs are barely covered in some land areas and the oceans. And LEO-BTM-based IPPs' coverage is a lot better than the GNSS-only-based one. It is getting more obvious with time getting longer. LEO-BTM has limited contribution to the IPP distribution with the length of time by 5 min. On the contrary, the number

of IPPs increases considerably with the length of time by 15 min. However, there are still many data gap areas shown in the subplot. For the IPPs of LEO-UP, it shows a much better distribution even during short observing session, and the density also increases to a certain extent, thus further improving the accuracy of ionospheric modeling. This is attributed to the fact that ionosphere monitoring based on GNSS-only and LEO-BTM highly depends on the number and the distribution of ground stations. In areas like some part of Africa, Antarctica, and the oceans, the lack of ground stations results in serious inadequacy of IPPs. Furthermore, the IPP distribution of LEO-UP seems to be good enough with the length of time by 5 min, which indicates that a great deal of data observed by LEO satellite constellation may provide a potential opportunity for real-time ionospheric modeling with high-temporal resolution and high accuracy if the observed data can be obtained in real time. Considering efficiency and feasibility, it is also of great importance to explore the optimal time length for modeling.

And that is where the LEO satellites contribute most to the IPP distribution compared with GNSS-only. This can be more clearly reflected in the following two areas. Figures 6 and 7 show the regional coverage of IPPs in polar region and Africa, respectively. The distribution of ground stations, IPPs of GNSS-only, and LEO of 192 satellites is represented by green, red, and blue dots, respectively. Due to the GNSS orbit inclination (55–65°), the IPP distribution in polar region is not very ideal even though the number of GNSS stations is very large. However, it is obvious that LEO satellite-based ionospheric observations have a better coverage

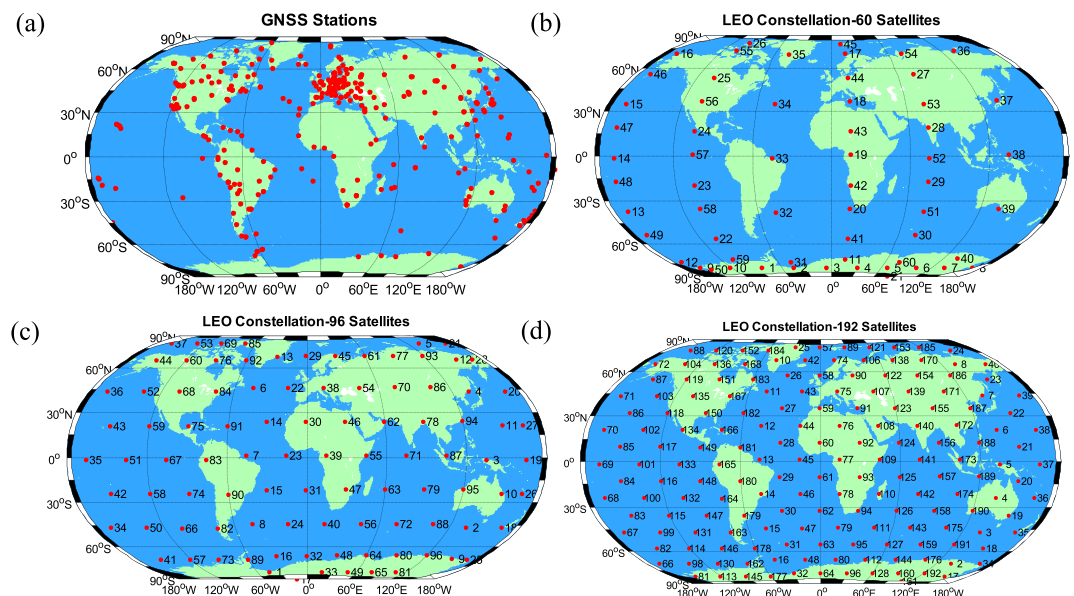


Figure 4. Distribution of ground-based Global Navigation Satellite System (GNSS) stations and Low-Earth-Orbiting (LEO) satellite-based stations with different LEO satellite number.

Table 3
Detailed Information for Ionosphere Model

Spacial range	Elevation cutoff	Fitting function	Spatial resolution	degree and order	Mapping function	Representation in the time domain	Sampling rate	Shell height
90°S–90°N, 180°W–180°E	10°	SH expansion	2.5°×5° (Latitude×Longitude)	15×15	MSLM	piece-wise function	linear 30 s	450 km

and higher density of IPPs in polar region because of the polar-orbiting satellites for most LEO constellations. In the Central African, the number of GNSS stations is relatively limited due to the harsh natural conditions. These areas cannot be observed with GNSS-only. From Figures 6 and 7, we can see that LEO constellation can significantly reduce the coverage of areas without GNSS observations.

Figure 8 presents the global coverage of IPPs with LEO satellite constellations of different satellite number. The length of observation time lasts 2 hr. The red dots represent IPPs with LEO-BTM, while the blue dots denote IPPs with LEO-UP. Obviously, with the increase of the number of LEO satellites, both the coverage and density of LEO-UP and LEO-BTM IPPs have a significant improvement. However, the improvement is no longer distinct when the number of LEO satellites exceeds 96. On the other hand, IPPs of LEO-UP are more evenly distributed than that of LEO-BTM because of the free limit of ground stations. Moreover, IPPs with LEO constellation of 60 satellites appear strip-like distribution. This is due to the fact that these LEO satellites are distributed in 6 polar-orbiting planes.

Figure 9 shows the density of IPPs based on GNSS-only and GNSS+LEO with different satellite cutoff elevations of 10, 20, and 40°, respectively. The left subfigures are related to GNSS-only, and the right ones are with GNSS+LEO. Compared with that of GNSS-only, the density of IPPs based on GNSS+LEO can be improved significantly. Even if the cutoff elevation is increased to 40°, the IPP density of GNSS+LEO is still better than that of GNSS-only at 10° especially in the oceans with approximately 200 more ionospheric observations in a grid (2.5° × 5°). This way the cutoff elevation angle of the GNSS measurements can be increased, since the mapping function error and the multipath effect are reduced.

3.3. Accuracy Assessment of Ionosphere Modeling

The aforementioned analyses show that LEO-augmented GNSS can improve the number and distribution of IPPs globally, which can improve the accuracy of the ionosphere models. In this part, to further verify the contribution of LEO observations in ionospheric modeling, we analyze the modeling results from the three solutions, that is, GNSS-only, GNSS combined with LEO-BTM (GNSS+LEO-BTM), and GNSS combined

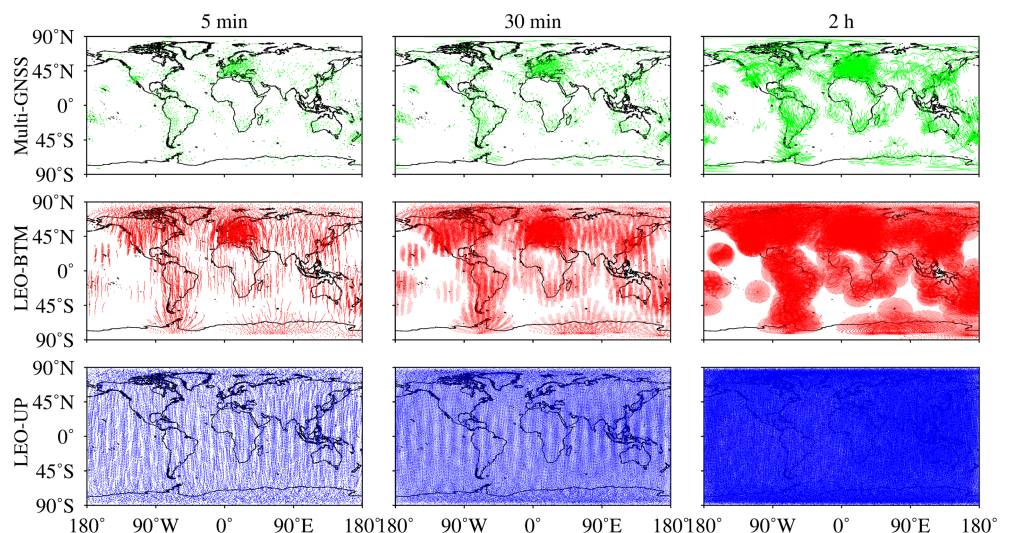


Figure 5. Distribution of ionospheric pierce points derived from Low-Earth-Orbiting (LEO) constellation with 192 satellites within different time spans, that is, 5 min, 30 min, and 2 hr, respectively.

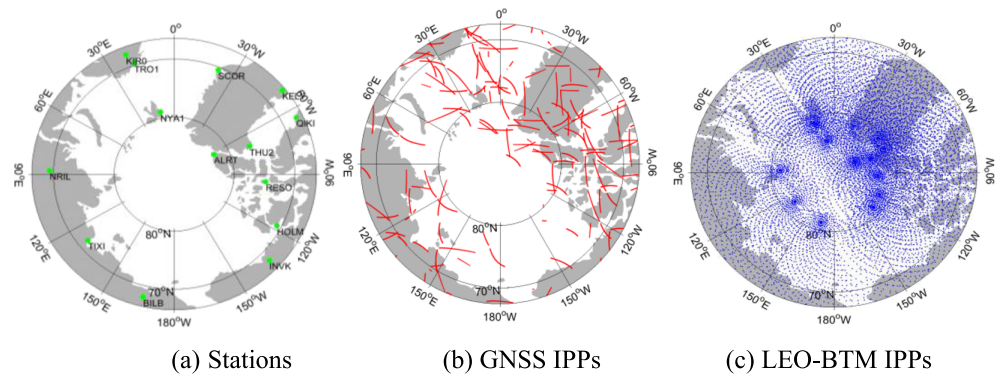


Figure 6. Distribution of monitoring stations and ionospheric pierce points (IPPs) derived from Global Navigation Satellite System (GNSS) and Low-Earth-Orbiting (LEO) over polar region.

with LEO-BTM and LEO-UP (GNSS+LEO-BTM+LEO-UP). Details of the modeling strategies are shown in Table 3.

To know the modeling results of different solutions, Figures 10a–10c show the global ionosphere maps based on GNSS-only, GNSS+LEO-BTM, and GNSS+LEO-BTM+LEO-UP solution every 2 hr on day of year (DOY) 001, 2017, respectively. It can be seen that all the three solutions are able to describe and characterize the temporal and spatial characteristics of the ionosphere and apparently have inherent consistency. The maximum TEC values of the three models are all over 40 total electron content unit (TECU).

It is hard to distinguish the difference of different global ionosphere models from the three solutions in Figure 10. In order to perform their difference and evaluate their accuracy, it is necessary to select the true reference ionosphere model. Considering ionospheric observations of GNSS and LEO satellites are simulated by applying IRI model, thus, the ionospheric TEC values calculated by IRI model can be used as true reference values, which are named as IRI-GIM in short. Then the difference between calculated GIMs and IRI-GIM can be used to describe the accuracy of TEC modeling with different system combinations, which is embodied in Figures 11–13.

As we can see from Figure 11, which shows the difference between GNSS-only and IRI model every 2 hr on DOY 001, 2017, the performance of GNSS-only is significantly worse in the southern hemisphere, oceans, and regions near the equator, especially in Pacific at 0:00 UTC and 2:00 UTC and central Africa between 16:00–22:00 UTC. The maximum deviation in these areas can reach around ± 6 TECU. This is due to the fact that during 0:00–2:00 UTC and 16:00–22:00 UTC, the ionospheric camel-back structure is temporarily located in the ocean area and central Africa, respectively (see Figure 10). However, there are none or few GNSS ground stations in these areas, resulting in limited number and uneven distribution of IPPs (see

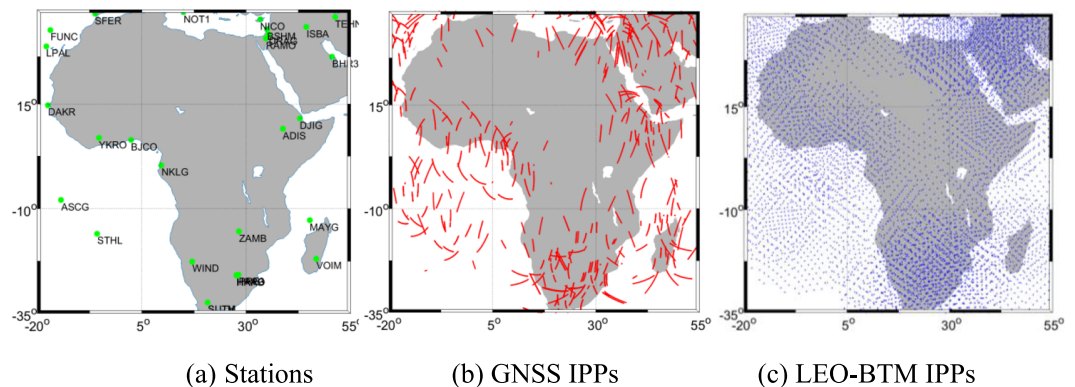


Figure 7. Distribution of monitoring stations and ionospheric pierce points (IPPs) derived from Global Navigation Satellite System (GNSS) and Low-Earth-Orbiting (LEO) over Africa.

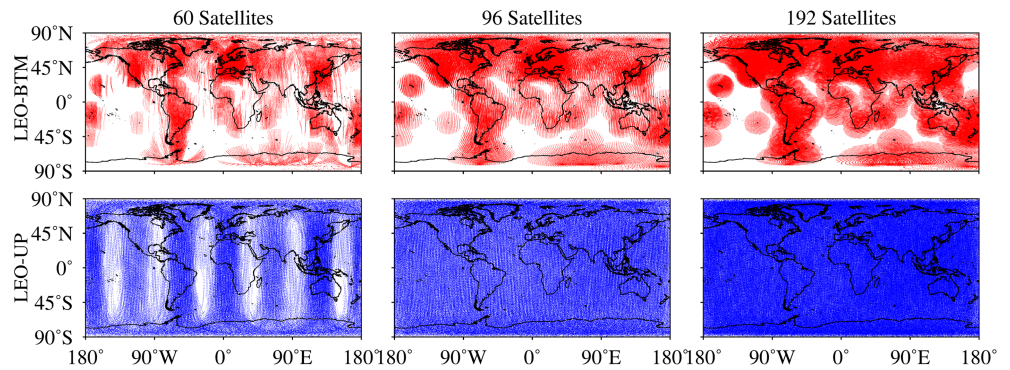


Figure 8. Distribution of ionospheric pierce points derived from different Low-Earth-Orbiting (LEO) constellations within 2 hr.

Figure 5), which makes the results of ionospheric modeling quite different from the actual ionospheric values. Figure 12 shows the accuracy of GNSS ionosphere model augmented by LEO-BTM every 2 hr on DOY 001, 2017. In this figure, the maximum of deviation is around ± 2 TECU. Compared with that of GNSS-only, GNSS augmented by LEO-BTM observations can improve the accuracy of ionosphere model by about 2 TECU on the whole. Besides, it has raised the accuracy remarkably in central Africa due to the abundant observations of LEO satellites. But the geographical coverage of improvement is still limited, because LEO-BTM observations can only expand the IPP coverage to a certain extent considering the limit of ground-based stations. Through comparing corresponding areas with those in Figure 13, we can see that the accuracy of ionosphere model is improved considerably after adding LEO-UP and LEO-BTM observations. However, there are strip-like errors near the equator and in the ocean area, which is probably caused by the degree and order of the chosen SH expansion.

To verify what causes the strip-like errors near the geomagnetic equator and over the oceanic region, different degree and order values of the SH expansions, namely, 8, 15, 20, and 30, have been chosen to model the global ionosphere, respectively. The differences between the ionospheric modeling results with different SH expansion orders and the reference values (IRI-GIM) are shown in the Figures 14a–14d, respectively. As we can see, when we use low-order SH expansion to model the ionosphere, that is, 8, the strip-like error is

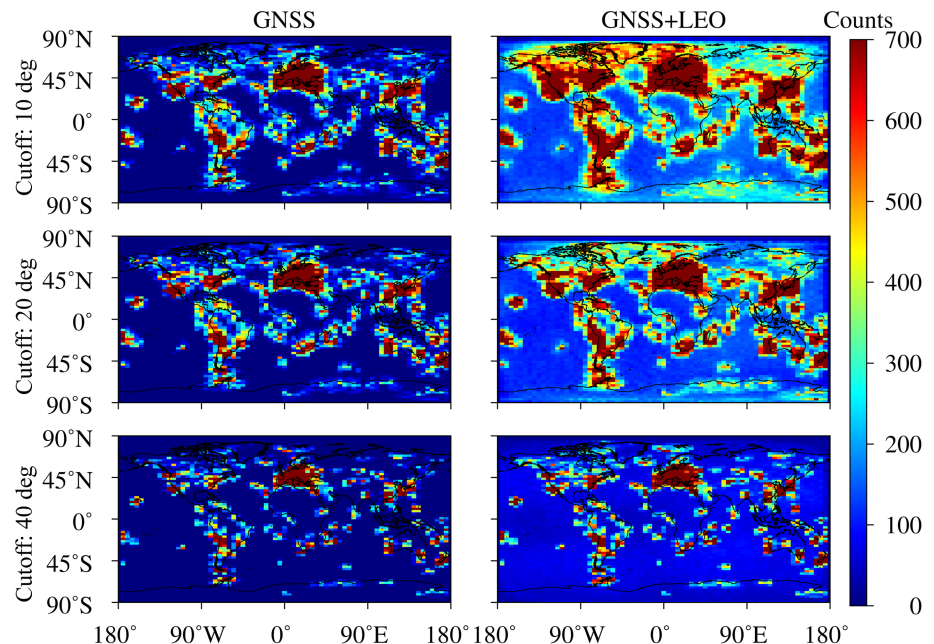
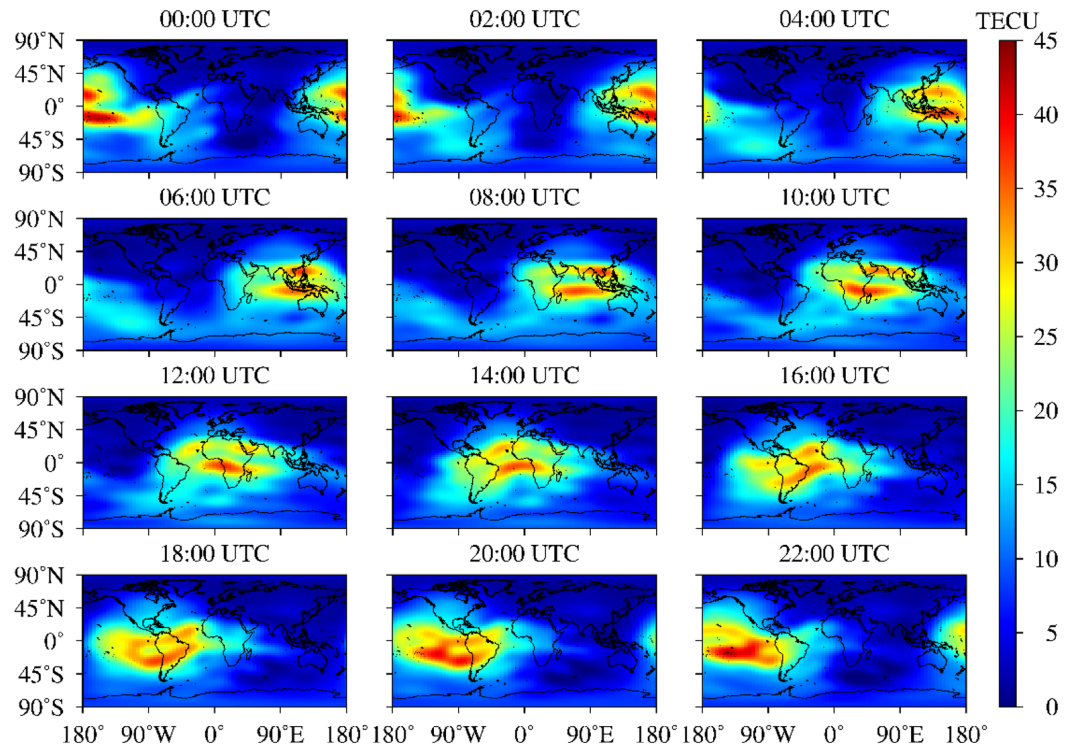
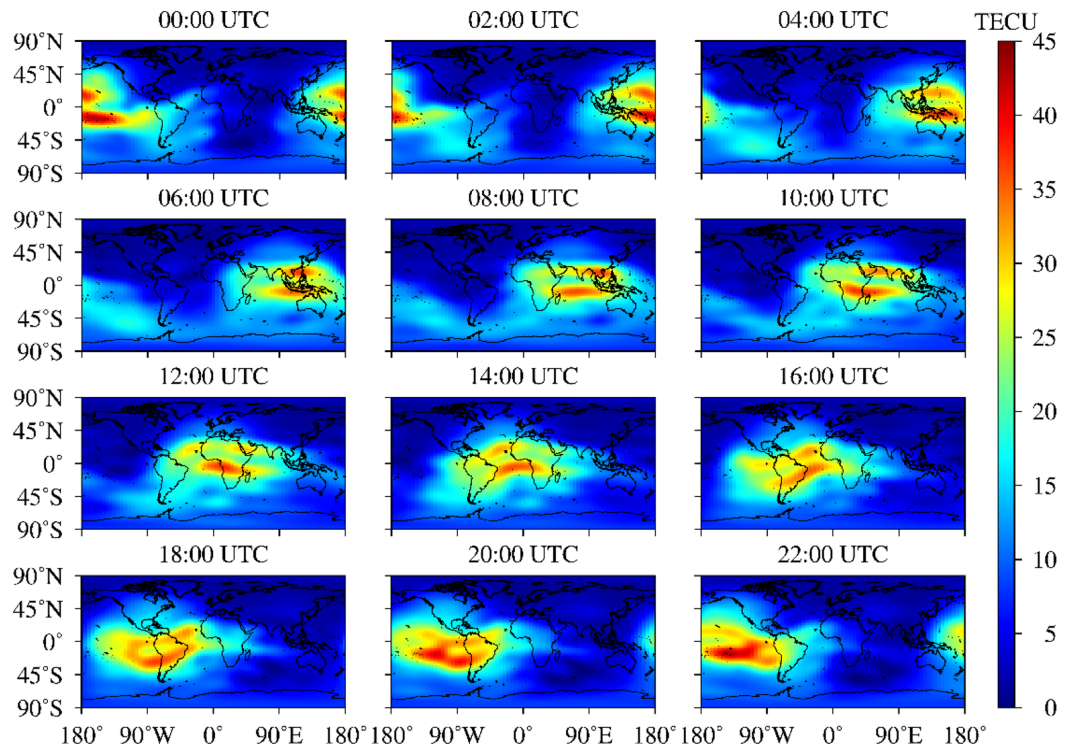


Figure 9. Density of ionospheric pierce point (IPP) derived from Global Navigation Satellite System (GNSS) and Low-Earth-Orbiting (LEO)-augmented GNSS with different cutoff elevations angles, namely, 10, 20, and 40°.



(a) GNSS-only



(b) GNSS+LEO-BTM

Figure 10. Global ionospheric maps derived from Global Navigation Satellite System (GNSS)-only, GNSS+LEO-BTM, and GNSS+LEO-BTM+LEO-UP every 2 hr on day of year 001, 2017 (Unit: total electron content unit [TECU]).

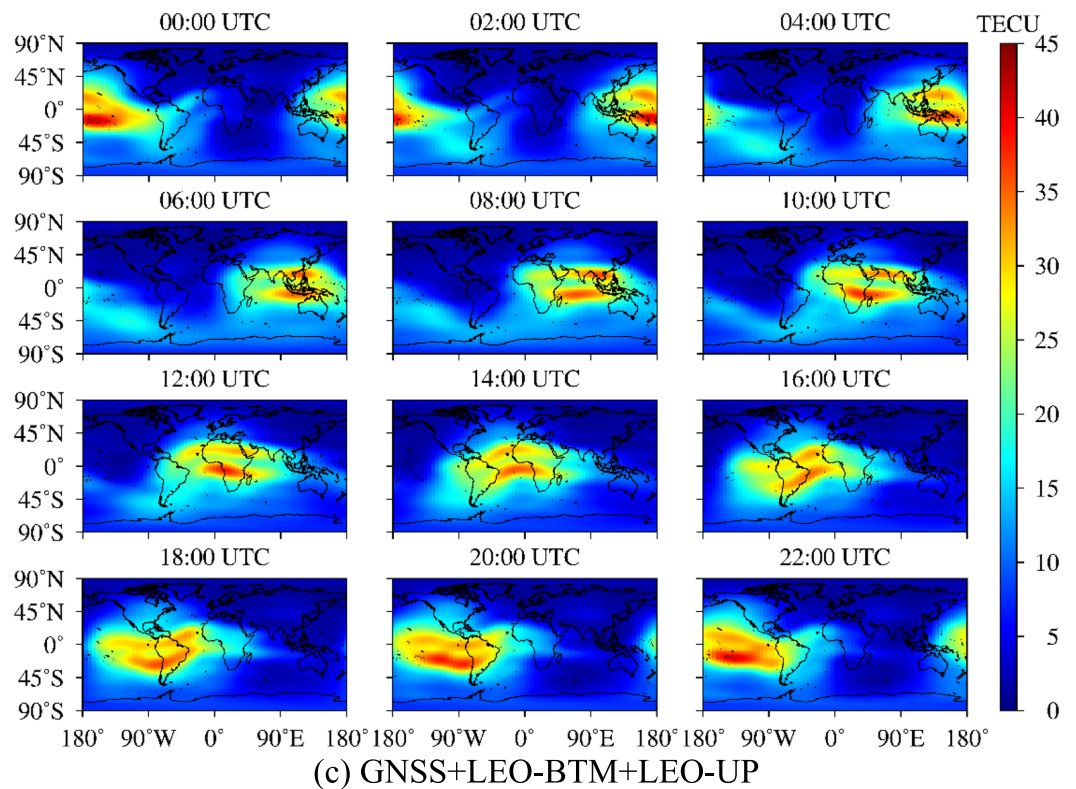


Figure 10. (continued)

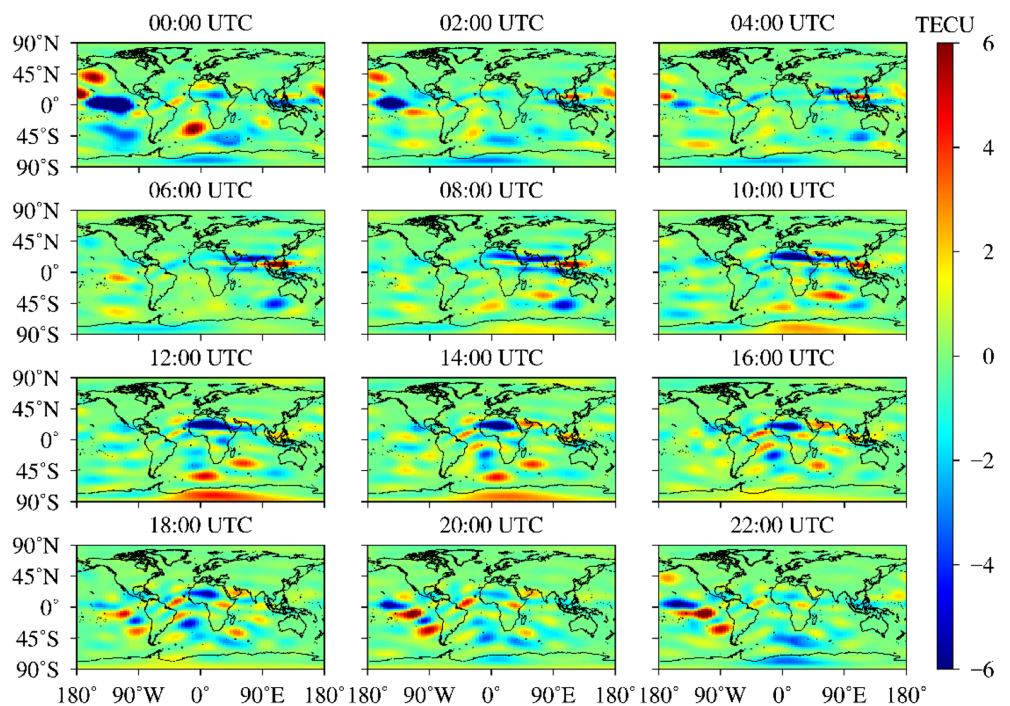


Figure 11. Differences between Global Navigation Satellite System (GNSS)-only and the International Reference Ionosphere model results every 2 hr on day of year 001, 2017 (Unit: total electron content unit [TECU]).

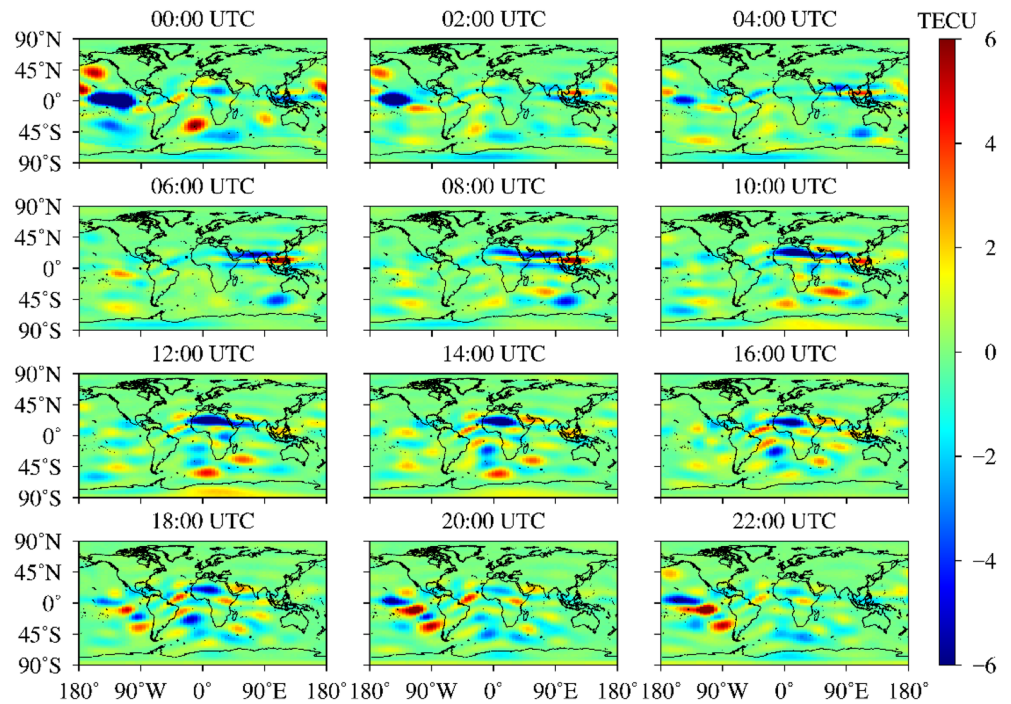


Figure 12. Differences between Global Navigation Satellite System (GNSS) augmented by LEO-BTM and International Reference Ionosphere model results on day of year 001, 2017 (Unit: total electron content unit [TECU]).

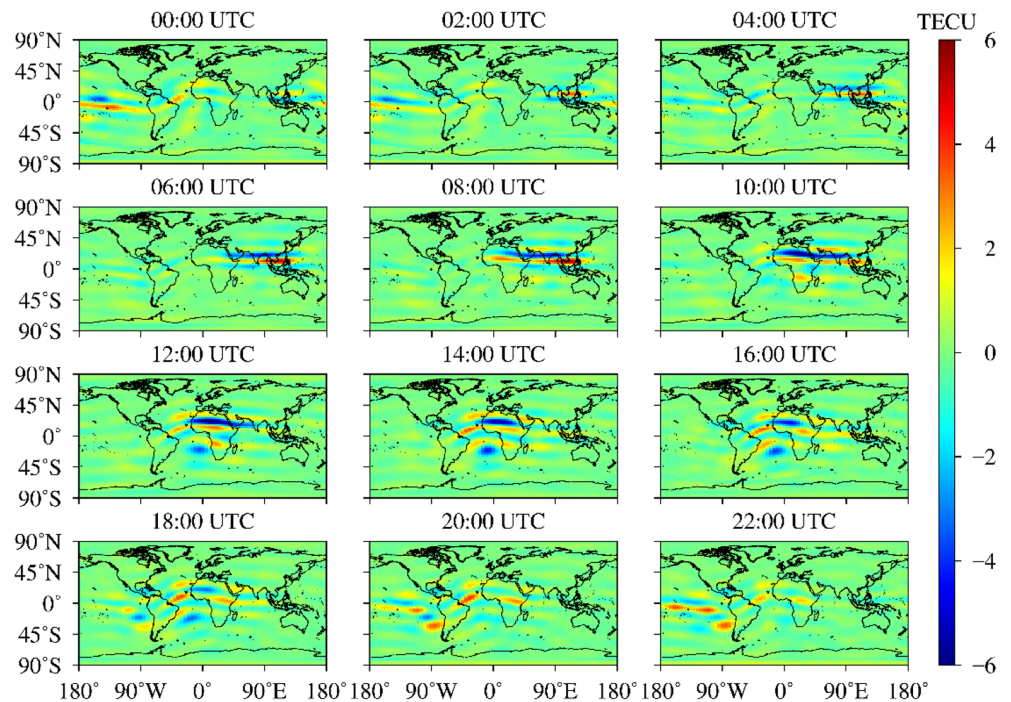
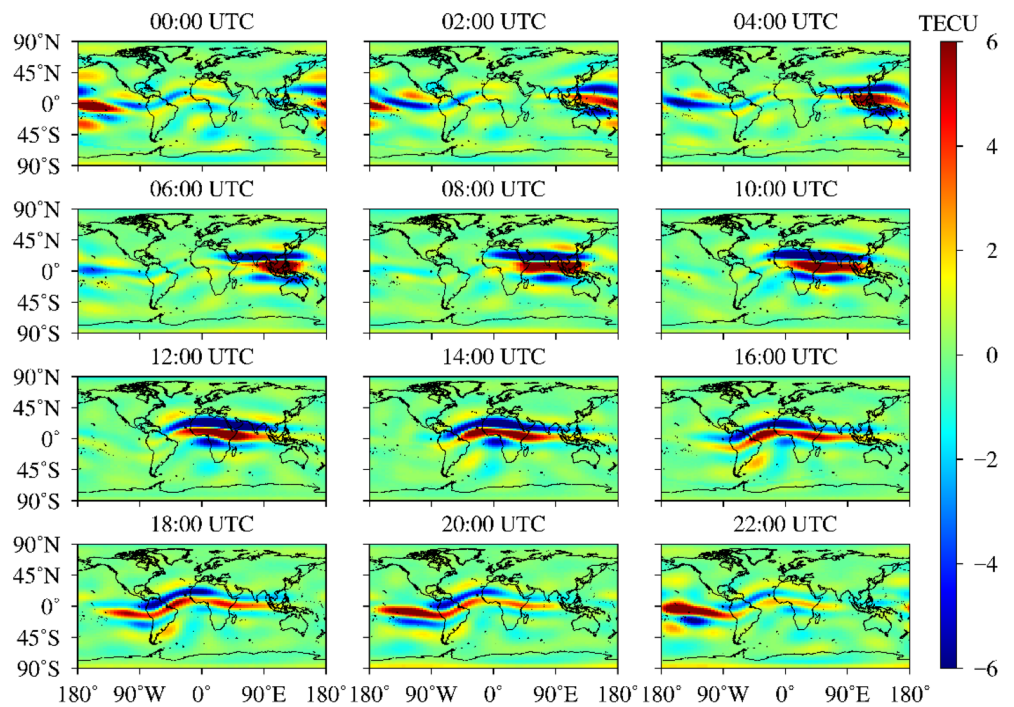
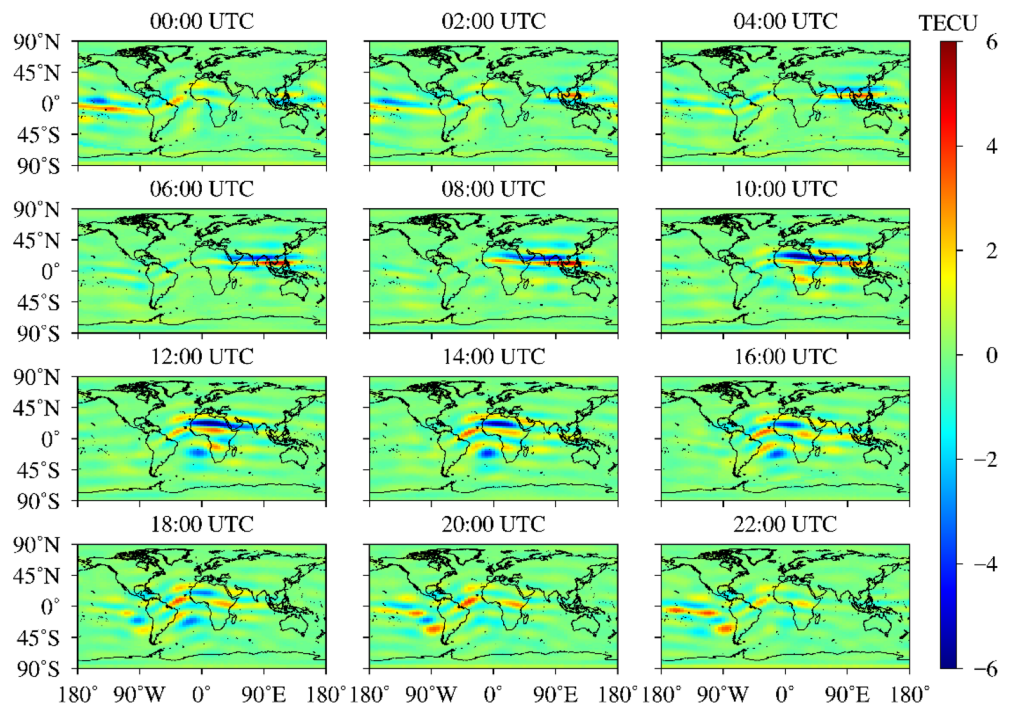


Figure 13. Differences between Low-Earth-Orbiting (LEO)-augmented Global Navigation Satellite System (GNSS) and International Reference Ionosphere model results on day of year 001, 2017 every 2 hr (Unit: total electron content unit [TECU]).



(a) 8×8 SH expansion



(b) 15×15 SH expansion

Figure 14. Accuracy of Global Navigation Satellite System (GNSS) + Low-Earth-Orbiting (LEO) global ionosphere model using spherical harmonics (SH) with different order and degree of 8, 15, 20, and 30 every 2 hr on day of year 001, 2017.

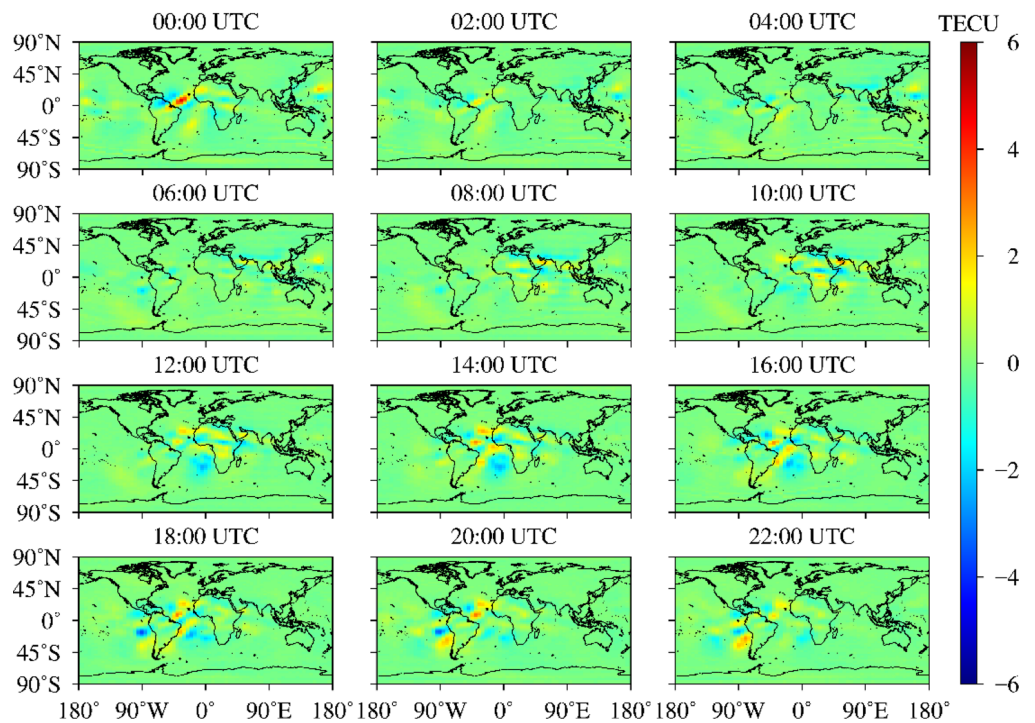
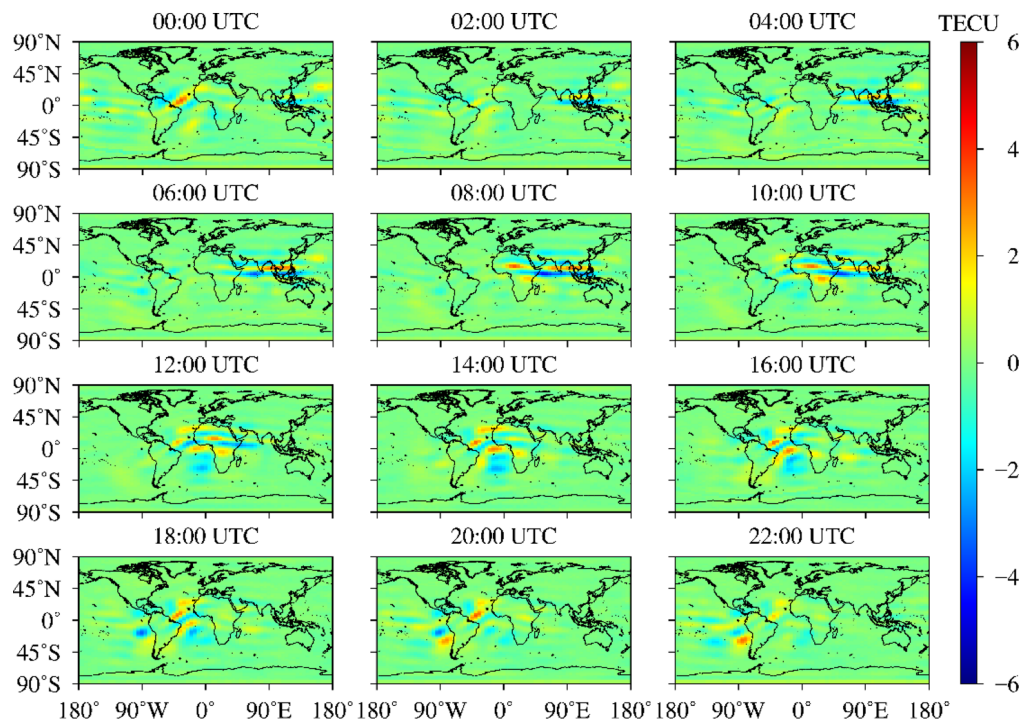


Figure 14. (continued)

obviously larger than that of other high-order SH expansion, that is, 15, 20, and 30. Besides, with the increase of SH expansion order, the accuracy of ionospheric modeling is also remarkably improved. Especially, when the degree and order of SH expansion is larger than 20, the strip-like errors almost disappear. Moreover, the maximum deviation is not more than 0.5 TECU. It can be seen that LEO satellite constellation provides more

Table 4
The Statistical Accuracy of Different Solutions Using 30-Day Data Between DOY 001–030, 2017

Systems	Models	Mean bias	Min bias	Max bias	<i>STD</i>	RMS	Improvement (%)
GNSS	G	−0.11	−18.1	12.6	1.13	1.14	-
LEO(60)	G+L	−0.02	−10.4	7.9	0.73	0.73	35.90
LEO(96)	G+L	−0.07	−8.2	7.2	0.61	0.61	46.50
LEO(192)	G+L	−0.06	−7.0	6.4	0.57	0.57	50.00

Note. Unit: TECU; G: GNSS; L: LEO.

Abbreviations: DOY: day of the year; GNSS: Global Navigation Satellite System; LEO: Low-Earth-Orbiting; RMS: root mean square; TECU: total electron content unit.

uniformly distributed ionospheric observations for global ionospheric modeling, which can not only improve the accuracy of ionospheric modeling but also provide the possibility of establishing a high spatial-resolution ionospheric model based on SH expansion with higher order.

To understand the difference between the different solutions and the IRI-GIM, we study the statistical results during 30 days as shown in Table 4, including bias, *STD*, RMS values, and the improvement of GNSS+LEO compared with that of GNSS-only. According to the results, it indicates that the accuracy of the ionosphere model of the LEO-augmented GNSS improves significantly compared with GNSS-only. To be more specific, the improvement of the model increases with the increasing number of LEO satellites. The minimum and maximum biases reduce from −18.1 TECU to −7.0 TECU and from 12.6 TECU to 6.4 TECU, respectively. Besides, *STD* and RMS also show clear improvement. The more LEO satellites, the more obvious the improvement of model accuracy. In terms of GNSS+LEO-BTM+LEO-UP, the RMS with LEO constellations of 60 and 96 satellites have been improved by 35.9% and 46.5%, respectively. Especially, with GNSS augmented by 192 satellite LEO constellation, the improvement can remarkably reach 50%.

4. Conclusions

This study is aimed at investigating the contributions and benefits made by LEO constellations to the performance of GNSS global ionospheric modeling. First, three LEO constellations of 60, 96, and 192 LEO satellites are typically designed. Together with multi-GNSS constellations, that is, GPS, GLONASS, BDS, and Galileo, we have simulated ionospheric observations by applying STK software and IRI model and then conduct the global ionosphere modeling. Finally, we assess LEO contributions by analyzing the performance of LEO-augmented GNSS ionospheric modeling in the aspects of IPP distribution and ionosphere model accuracy. After the above discussion, the following conclusions can be drawn:

1. In terms of IPP distribution, LEO constellation can expand the coverage and increase the density of IPPs, effectively filling the data gap in some areas, where IPPs derived from GNSS are limited by the number and distribution of ground tracking stations globally, especially in the oceans, polar region, and part of Africa. And with the prolongation of observation time and more LEO satellites, the IPP coverage shows more considerable expansion. Based on 192 LEO satellites, LEO-based observations have a uniform distribution globally even with the short length of time by 5 or 15 min, which is of great significance for real-time ionospheric modeling. Additionally, the IPP density of GNSS+LEO when the cutoff elevation is set to 40° is better than that of GNSS-only at 10°, especially in the oceans with approximately 200 more IPPs within a grid (2.5° × 5°). This way the cutoff elevation angle of the GNSS measurements can be increased, since the mapping function error and the multipath effect are reduced. It is beneficial to improve the accuracy of ionospheric model by increasing the cutoff elevation.
2. As for the accuracy of ionosphere model, based on the GNSS-only solution and GNSS+LEO solution, the modeling performances of these solutions are evaluated. For GNSS+LEO solution using 30-day data, the RMS with LEO constellations of 60, 96, and 192 satellites have been improved by 35.9%, 46.5%, and 50%, respectively, compared with that of GNSS-only. And the minimum and maximum biases of ionosphere model using GNSS+LEO solution can be reduced from −18.1 to −7.0 TECU and from 12.6 to 6.4 TECU, respectively.

Finally, we want to mention that this paper mainly focuses on the LEO contributions to ionosphere modeling in an optimal situation, where the simulated observations do not consider errors, such as observation

noise, code/phase hardware delays, and multipath effects. To conduct further research, we will simulate more realistic observations and analyze the impact of different types of errors on the ionospheric modeling results. Besides, considering different LEO constellations have different ionospheric detectable ranges due to their different orbital altitudes, how to make full use of LEO and GNSS observations to achieve the optimal data fusion is a key issue to build a high-precision and high-resolution ionospheric model. All these will be studied in the next step.

Acknowledgments

This research was funded by the National Science Fund for Distinguished Young Scholars (grant 41825009), the National Natural Science Foundation of China (no. 41904026), the Hubei Province Natural Science Foundation of China (2018CFA081), the National Youth Thousand Talents Program, the Funds for Creative Research Groups of China (grant 41721003), the National Key Research and Development Program of China (2016YFB0501803 and 2017YFB0503402), the project of Wuhan Science and Technology Bureau (2018010401011270), Chinese Academy of Sciences, Key Laboratory of Geospace Environment, University of Science & Technology of China, Key Laboratory of Geospace Environment and Geodesy, Ministry of Education, Wuhan University (no. 18-02-02) and Guangxi Key Laboratory of Spatial Information and Geomatics (no.17-259-16-05). The numerical calculations have been done on the supercomputing system in the Supercomputing Center of Wuhan University. We are very grateful to the IRI Working Group for providing the IRI model code in Fortran from the IRI homepage at irimodel.org and the Crustal Dynamics Data Information System (CDDIS) data center for providing observation data and navigation file by the following FTP server: <ftp://cddis.gsfc.nasa.gov/pub/gps/data/daily/>. In addition, we also gratefully acknowledged the use of Generic Mapping Tool (GMT) software and Matlab 2016 software.

References

- Abdelazeem, M., Çelik, R. N., & El-Rabbany, A. (2017). An efficient regional ionospheric model using combined GPS/BeiDou observations. *Journal of Spatial Science*, *62*(2), 323–335. <https://doi.org/10.1080/14498596.2016.1253512>
- Alizadeh, M. M., Schuh, H., Todorova, S., & Schmidt, M. (2011). Global ionosphere maps of VTEC from GNSS, satellite altimetry, and Formosat-3/COSMIC data. *Journal of Geodesy*, *85*(12), 975–987. <https://doi.org/10.1007/s00190-011-0449-z>
- Billitz, D., Altadill, D., Truhlik, V., Shubin, V., Galkin, I., Reinisch, B., & Huang, X. (2017). International Reference Ionosphere 2016: From ionospheric climate to real-time weather predictions. *Space Weather*, *15*, 418–429. <https://doi.org/10.1002/2016SW001593>
- Chen, P., Yao, Y., & Yao, W. (2017). Global ionosphere maps based on GNSS, satellite altimetry, radio occultation and DORIS. *GPS Solutions*, *21*(2), 639–650.
- Dettinger, D., Limberger, M., & Schmidt, M. (2014). Using DORIS measurements for modeling the vertical total electron content of the Earth's ionosphere. *Journal of Geodesy*, *88*(12), 1131–1143.
- Feltens, J., & Schaer, S. (1998). *IGS products for the ionosphere, proceedings of the IGS Analysis Center Workshop* (pp. 225–232). Germany: ESA/ESOC Darmstadt.
- Hanson, W. A. (Ed.) (2016). In their own words: Oneweb's internet constellation as described in their fcc form 312 application. *New Space*, *4*(3), 153–167. <https://doi.org/10.1089/space.2016.0018>
- Hernández-Pajares, M., Juan, J. M., Sanz, J., Aragón-Ángel, A., García-Rigo, A., Salazar, D., & Escudero, M. (2011). The ionosphere: Effects, GPS modeling and the benefits for space geodetic techniques. *Journal of Geodesy*, *85*(12), 887–907.
- Hu, A., Li, Z., Carter, B., Wu, S., Wang, X., Norman, R., & Zhang, K. (2019). Helmert-VCE-aided fast-WTLS approach for global ionospheric VTEC modelling using data from GNSS, satellite altimetry and radio occultation. *Journal of Geodesy*, *93*(6), 877–888.
- Kumar, S. (2016). Performance of IRI-2012 model during a deep solar minimum and a maximum year over global equatorial regions. *Journal of Geophysical Research: Space Physics*, *121*, 5664–5674. <https://doi.org/10.1002/2015JA022269>
- Lanyi, G. E., & Roth, T. (1988). A comparison of mapped and measured total ionospheric electron content using global positioning system and beacon satellite observations. *Radio Science*, *23*(4), 483–492. <https://doi.org/10.1029/RS023i004p00483>
- Lawrence, D., Cobb, H. S., Gutt, G., Tremblay, F., Laplante, P., & O'Connor, M. (2016). Test results from a LEO-satellite-based assured time and location solution. In *Proceedings of the 2016 International Technical Meeting of the Institute of Navigation*, Monterey, CA, USA (pp. 25–28).
- Li, H., Yuan, Y., Li, Z., Huo, X., & Yan, W. (2012). Ionospheric electron concentration imaging using combination of LEO satellite data with ground-based GPS observations over China. *IEEE Transactions on Geoscience and Remote Sensing*, *50*(5), 1728–1735.
- Li, X., Ma, F., Li, X., Lv, H., Bian, L., Jiang, Z., & Zhang, X. (2019). LEO constellation-augmented multi-GNSS for rapid PPP convergence. *Journal of Geodesy*, *93*(5), 749–764.
- Mannucci, A. J., Wilson, B. D., & Edwards, C. D. (1993). A new method for monitoring the Earth ionosphere total electron content using the GPS global network paper presented at ION GPS 93, Inst. Of Navig., Salt Lake City, Utah.
- Nava, B., Coisson, P., & Radicella, S. M. (2008). A new version of the NeQuick ionosphere electron density model. *Journal of Atmospheric and Solar-Terrestrial Physics*, *70*(15), 1856–1862.
- Reid, T. G., Neish, A. M., Walter, T. F., & Enge, P. K. (2016). Leveraging commercial broadband LEO constellations for navigation. In *Proceedings of the ION GNSS* (pp. 2300–2314).
- Ren, X., Chen, J., Li, X., Zhang, X., & Freeshah, M. (2019). Performance evaluation of real-time global ionospheric maps provided by different IGS analysis centers. *GPS Solutions*, *23*(4), 113. <https://doi.org/10.1007/s10291-019-0904-5>
- Ren, X., Zhang, X., Xie, W., Zhang, K., Yuan, Y., & Li, X. (2016). Global ionospheric modelling using multi-GNSS: BeiDou, Galileo, GLONASS and GPS. *Scientific Reports*, *6*(1), 33,499. <https://doi.org/10.1038/srep33499>
- Schaer, S. (1999). Mapping and predicting the Earth's ionosphere using the Global Positioning System. 1999. 205p (Doctoral dissertation, Ph. D. dissertation. University of Bern, Bern, Switzerland).
- Selding, P. B. (2015a). SpaceX to build 4,000 broadband satellites in Seattle. *Space News*, *19*.
- Selding, P. B. (2015b). Virgin qualcomm invest in OneWeb satellite Internet venture. *Spacenews*.
- Selding, P. B. (2016). Boeing proposes big satellite constellations in V-and C-bands. *Space News*, *23*.
- Todorova, S., Hobiger, T., & Schuh, H. (2008). Using the Global Navigation Satellite System and satellite altimetry for combined global ionosphere maps. *Advances in Space Research*, *42*(4), 727–736.
- Wang, C., Xin, S., Liu, X., Shi, C., & Fan, L. (2018). Prediction of global ionospheric VTEC maps using an adaptive autoregressive model. *Earth, Planets and Space*, *70*(1), 18. <https://doi.org/10.1186/s40623-017-0762-8>
- Yao, Y., Liu, L., Kong, J., & Zhai, C. (2018). Global ionospheric modeling based on multi-GNSS, satellite altimetry, and Formosat-3/COSMIC data. *GPS Solutions*, *22*(4), 104. <https://doi.org/10.1007/s10291-018-0770-6>
- Yuan, Y., & Ou, J. (2002). Differential areas for differential stations (DADS): a new method of establishing grid ionospheric model. *Chinese Science Bulletin*, *47*(12), 1033–1036. <https://doi.org/10.1007/BF02907577>
- Zhang, R., Song, W. W., Yao, Y. B., Shi, C., Lou, Y. D., & Yi, W. T. (2015). Modeling regional ionospheric delay with ground-based BeiDou and GPS observations in China. *GPS Solutions*, *19*(4), 649–658.